

4

CONF

THE EFFECT OF DISSOLVED OZONE ON THE CORROSION
BEHAVIOR OF Cu-30 Ni AND 304L STAINLESS STEEL
IN 0.5 N NaCl SOLUTIONS

H.H. Lu and D.J. Duquette
Rensselaer Polytechnic Institute
Materials Engineering Department
Troy, New York 12180-3590

OCTOBER 1989

Technical Report to the Office of Naval Research

Contract No. N00014-89-J-1125

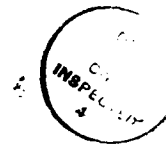
AD-A213 804

Reproduction in whole or in part for any purpose of the U.S.
Government is permitted. Distribution of this document is
unlimited.

a

023

The Effect of Dissolved Ozone on the Corrosion
 Behavior of Cu-30 Ni and 304L Stainless Steel
 in 0.5 N NaCl Solutions



H.H. Lu and D.J. Duquette
 Materials Engineering Department
 Rensselaer Polytechnic Institute
 Troy, New York 12180-3590

Accession For	
NTIS GRA&I	<input checked="" type="checkbox"/>
DTIC TAB	<input type="checkbox"/>
Unannounced	<input type="checkbox"/>
Justification	
By _____	
Distribution/	
Availability Codes	
Dist	Avail and/or Special
A-1	

ABSTRACT

Cu-30 Ni - 30% Pickle

Electrochemical experiments on the effect of dissolved ozone on the corrosion behavior of Cu-30 Ni and 304 L stainless steel have been performed in 0.5 N NaCl solutions at room temperature. The experiments performed included measurements of corrosion potential as a function of time and ozone concentrations, cyclic polarization experiments, iso-potential measurements of current densities and Auger electron spectroscopy studies of the chemical composition of the corrosion product films. The results of these experiments have shown that for both the Cu-based alloy and the stainless steel, the corrosion potential exhibits a marked shift to more noble values (≈ 300 mv) for ozone concentrations less than 0.2 - 0.3 mg/l. At higher ozone concentrations the corrosion potential is virtually independent of the level of ozone dissolved in the solution. In addition to the shift in the corrosion potential, the presence of dissolved ozone resulted in a reduction in the corrosion rate for the Cu-30 Ni alloy, as measured by a significant decrease in the current density at a constant applied potential. This improvement in the corrosion resistance appears to be related to a reduction in the corrosion product film thickness and a higher fraction of oxygen to chloride in the corrosion product film.

For the stainless steel, ~~on the other hand~~, Auger electron spectroscopy indicated no appreciable differences between the passive film produced in ozonated solutions versus those in unozonated solutions. However, the noble shift in the corrosion potential was accompanied by a parallel shift in the breakdown potential, suggesting that films produced

in ozonated solutions are more resistant to the initiation of localized corrosion. However, the repassivation potential of the stainless steel is not perceptably changed by dissolved ozone and the corrosion potential approached the repassivation potential. This results in the rapid propagation of pits once they have initiated.

**The Effect of Dissolved Ozone in the Corrosion
Behavior of Cu - 30 Ni and 304 L Stainless
Steel in 0.5 N NaCl Solutions**

H.H. Lu and D.J. Duquette
Materials Engineering Department
Rensselaer Polytechnic Institute
Troy, New York 12180-3590

Introduction

Traditionally, chloride, or hypochlorite are utilized as biocides in aqueous solutions to control bio-fouling, bio-corrosion or the other biological activity on metal surfaces. However, dissolved chlorine is highly corrosive to a number of engineering alloys.⁽¹⁻⁶⁾ Additionally gaseous chlorine is highly dangerous, and the storage of hypochlorites is difficult because of their strong oxidizing tendency. An alternate method of controlling algae or other marine growth on heat exchanger surfaces is the use of ozone. Ozone is readily generated from air, is generally non-toxic to humans at the levels required to control algae and bacteria, and requires no storage capabilities. However, ozone is considered to be a strong oxidant and accordingly, when dissolved in water, may act as an accelerant of corrosion processes. For example, it has been shown that the corrosion rates of carbon and low alloy steels is increased by a factor of 2-3, while that of copper and brass is increased by a factor of 5-6 with -2ppm ozone dissolved in stagnant deionized water.⁽⁷⁾

Accordingly a study of the effects of ozone on the corrosion behavior of two alloys, a 70-30 Ni alloy, and a 304 L stainless steel alloy have been undertaken.

The two alloys were selected on the basis of the differences in electrochemical behavior of each. The Cu-Ni alloys is considered to be an "active" alloy which does not demonstrate electrochemical passivity, but rather depends on the properties of a dense, adherent, corrosion product film to inhibit rapid corrosion in near neutral aqueous solutions. The stainless steel, on the other hand is a classic example of an alloy which depends on a thin, transparent "passive" film to render protection against general corrosion. However, this alloy is well known to suffer from localized corrosion, by breakdown of the passive film, in halogenated waters. The breakdown of this passivity is related to a critical electrochemical potential, and strongly oxidizing environments may shift the naturally occurring corrosion potential above this critical potential and thus initiate pitting or other forms of localized corrosion.

Experimental Procedure

The alloys used in this study were a commercial cupro-nickel alloy nominally containing 70% Cu and 30% Ni. The exact composition of the alloy is shown in Table I. The second alloy studied was a 304 L stainless steel in the solution annealed condition. Its composition is also shown in Table I. The aqueous solutions utilized in the study were 0.5 N NaCl solutions acidified to pH5 with HCl at room temperature ($25 \pm 3^\circ\text{C}$). The test solutions were either deaerated by bubbling argon through the solution for two or more hours or were ozonated to different levels using a commercial ozone generator. The dissolved ozone concentration was

maintained at constant levels ranging from 0 to 2.5 ml/liter.

Samples for electrochemical polarization studies were mounted in epoxy resin mounts, wet ground to 600 grit SiC and rinsed with distilled water prior to testing.

Samples utilized for measuring current density as a function of time of exposure at constant potential were supported on a platinum tripod in order to avoid crevice corrosion.

Ozone was bubbled into the previously deaerated solution using a commercial ozonator which utilized air, supplied from an air pump, to produce the ozone. The ozone levels were measured for each experiment using the standard DPD method.⁽⁸⁾

The experiments performed included a measurement of the free corrosion potential as a function of time (to 4000 seconds) and cyclic voltametry at 10 mv/sec beginning at a potential of 100 mv. below the free corrosion potential. Each sample was held at a potential of -1.0 v vs SCE for five minutes prior to conducting the voltametry experiments, and the samples were initially polarized in the anodic direction. For the stainless steel alloy the pitting or breakdown potential, E_b , and the repassivation potential, E_p , were measured using the conventional criterion of a monotonic increase in the current with increasing anodic polarization for the former, and the re-establishment of passivity with increasing cathodic polarization for the latter. No breakdown potential was observed for the copper alloy.

In addition to potentiodynamic polarization experiments, a number of constant potential experiments were performed on each of the alloys to determine the variation of current density with time of exposure as a

function of applied potential. All electrochemical experiments were performed in triplicate.

The surfaces of the potentiodynamic experiment samples were examined after exposure to different dissolved ozone concentrations in the solution. Elemental concentration profiles through the corrosion product films were obtained using Auger Electron spectrometry (AES) in conjunction with argon ion sputtering.

Results

Corrosion Potential

Figure 1 shows the corrosion potential of the Cu-Ni alloy as a function of time. In the absence of ozone the corrosion potential rises rapidly and reaches a stable potential of -300 mv vs. SCE. Ozone additions tend to stabilize the corrosion potential at approximately 100 mv noble to that observed unozonated solutions and, except for a brief excursion in the noble direction for a solution containing 2 mg/liter ozone, the corrosion potential is only slightly dependent of ozone concentrations in excess of 0.06 mg/l. In addition, the transient period to stabilize the corrosion potential is essentially eliminated when ozone is present.

The average values of corrosion potential at the termination of these experiments (4000 sec) are shown in figure 2 and indicate a sharp rise in potential for low concentrations of ozone, followed by a gradual decrease in potential as the ozone concentration is increased.

Figure 3a and 3b show the corrosion potential as a function of ozone concentration and time for the 304L stainless steel alloy. The lowest concentration of ozone (0.015 mg/l) yielded essentially the same corrosion

potential as a sample immersed in the chloride solution with no ozone present. However, the transient period to achieve a stable corrosion potential essentially disappears with dissolved ozone. At all higher concentration of ozone, the corrosion potential is essentially constant, except for some variation at low concentration (< 0.5 mg/l). However, the stability of the corrosion potential for all but the lowest concentration of ozone is highly variable, particularly early in the experiment. The average value of the corrosion potential at the end of the experiments (4000 sec) is shown in figure 4 and indicates that the corrosion potential reaches a peak at approximately 0.2 mg/l, and then attains a constant value for higher concentrations of ozone.

Cyclic Polarization

Figure 5 shows typical cyclic polarization curves for the Cu-Ni alloy as a function of ozone concentration. Only the data for 0, 0.06 and 2.0 mg/l ozone are shown for clarity. Within the limits of reproducibility all of the curves are similar except that the data for the solution containing no ozone shows a more negative zero current potential (which mimicks the corrosion potential data). Also the limiting current density for anodic dissolution in the solutions containing ozone are generally somewhat less for the solution containing ozone, particularly on cathodic polarization.

Figure 6 shows typical cyclic polarization curves for the 304 L stainless steels in solutions containing ozone. For the most part the polarization curves of solutions containing greater than 0.15 mg/l ozone are virtually identical, and only the curves for 0, 0.016, and 2.0 mg/l ozone are shown for clarity. The addition of 0.016 mg/l ozone to the

solution had no observable effect on the zero current potential of the steel during anodic polarization confirming the results obtained for the steady state corrosion potential as a function of the concentration of ozone. However, the zero current corrosion potential at lower concentrations of ozone, is shifted approximately 200-300 mv in the noble direction. In addition to measuring the zero current potentials from these plots, the breakdown, or pitting potential (E_b) and the repassivation potentials (E_p) were also derived from the data. These data are shown in figure 7 and indicate that small amounts of ozone added to the solution result in a marked increase in the breakdown potential, to a value -300 mv noble to that observed in the absence of ozone. For ozone concentrations greater than -0.2 mg/l, the breakdown potential is essentially constant. With reference to the repassivation potential on the other hand, small amounts of ozone have little effect on E_p . However, there is an interesting active shift in E_p in the ozone concentration range of 0.2 - 0.5 mg/l range. At higher concentrations the repassivation potential is unchanged, and is essentially identical to that observed in the absence of ozone. When the corrosion potential is also plotted on the diagram it is interesting to note that active shift in repassivation potential is also mirrored in the breakdown potential, and in the corrosion potential. Moreover, in this range of ozone concentrations the corrosion potential and the repassivation potential are virtually identical and are separated by a few tens of millivolts at high ozone concentrations.

iso-Potential Currents

Figure 8 shows a current density vs. time plot for the Cu-Ni alloy as

a function of ozone concentration of the solution at an applied potential of 100 mv vs. SCE, which is in the limiting current density region of the polarization curve. In each case the current density decreases with time, indicating that the corrosion rate decreases with time of exposure. However, the steady state current density values for the copper based alloy is lower for the ozonated solution, indicating that the corrosion product film on the alloy is more protective under these conditions.

Similar data were collected for the stainless steel at a potential of +150 mv vs. SCE, and are shown in figure 9. This potential is between the breakdown potential and the repassivation potential. In virtually every case the current density exhibits instability when the potential was stepped from the corrosion potential to +150 mv vs SCE. However, after 2-5 minutes the current density monotonically increased and reached a stable value after 20-30 minutes. It appears that the current densities for the alloy in the ozonated solution were consistantly higher than that of the samples in the non-ozonation solution. However, the current densities are sufficiently small that it doubtful that the apparent increase is meaningful. A similar experiment performed at +100 mv vs. SCE showed similar results, however some samples in ozonated solutions showed lower as well as higher steady state current densities than those exposed to non-ozonation solutions. The data obtained at +100 mv vs SCE are similar to those obtained at +150 mv SCE, in that considerable instability was observed at the start of the experiment followed by a monotonic rise in current density to a steady state value of about the same order of magnitude as was observed at +150 mv vs. SCE. Mild pitting was observed on all samples at the conclusion of the experiments.

Surface Analyses

Auger electron spectroscopic analyses of the corrosion products of the copper alloy are shown in figure 10 for samples polarized in 0, 0.06, and 2.0 mg/l ozone solutions. In the absence of the ozone the surface of the alloy contains primarily Cu and Ni with a high percentage of chloride, which approaches zero at approximately 250 minutes of Auger sputtering. Trace amounts of iron were also detected in the film. The oxygen profile is similar to the chlorine profile in that it approaches zero after approximately 250 minutes of Argon sputtering. The Auger data from the samples exposed to the ozonated solution are similar to each other, but considerably different from the samples exposed to the non-ozonated solutions in that oxygen and chlorine concentrations are both initially high at the surface, but both concentrations decrease rapidly as the surface is sputtered, reaching essentially zero in ~80 minutes. The relative percentages of Cu and Ni incorporated into the film are virtually unchanged in the ozonated solutions when compared with the non-ozonated solution.

Auger electron spectroscopy data taken from the stainless steel samples, are shown in figure 11. These data indicate that neither the thickness or chemistry of the passive film on stainless steel are appreciably affected by the presence of ozone in the solution.

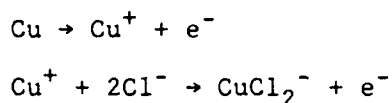
Dissussion

Cu-Ni Alloy

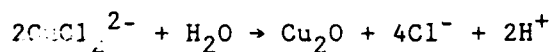
The results of this study indicate that ozonation of chloride solutions results in a marked shift of the corrosion potential in the active direction for Cu-Ni alloys. Except for minor changes in the

limiting current density, the short term electrochemical response of the alloy is virtually independent of the ozone concentration of the solution. However, long term exposure of the samples indicates that the alloy exposed to the ozonated solutions exhibits a lower current density response and that ozonated solutions result in lower corrosion rates. The AES data indicate that the corrosion product film for the samples exposed to the ozonated solutions is in fact thinner, although the general chemical composition of the film appears to be similar for both ozonated and non-ozonated solutions.

An examination of the potential -pH diagram for copper in chloride solutions (fig. 12) indicates that the corrosion of copper in the potential and pH range of the solution examined in this study occurs by the production of the monovalent copper ion, Cu^+ , and that this ion complexes with chloride according to the following reaction:



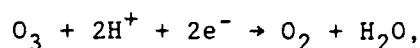
The solid Cu_2O then forms by hydrolysis of the CuCl_2^- complex:



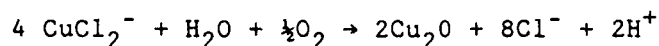
This reaction is autocatalytic with respect to the Cu in at the alloy surface, also results in the acidification of the solution immediately adjacent to the surface. It is likely that the nickel in the alloy oxidizes in a similar manner except that it does not form the complex but is converted directly to a form of NiO. Thus the amount of chlorine

detected in the AES analysis shows a very steep concentration gradient from the outer surface to the alloy surface. In the absence of ozone the chlorine signal maintains a steep concentration gradient, while the oxygen signal shows a relatively flat gradient, indicating that the conversion of CuCl^- to Cu_2O occurs within film.

When ozone is dissolved in the solution however, the reduction of the ozone as the cathodic reaction occurs accordingly to the following reaction:



and the hydrolysis reaction is assisted by the generation of O_2 accordingly to the reaction



This hypothesized reaction explains the dramatic shift in the corrosion potential in the noble direction, even with small amounts of ozone. Also this hypothesis explains the thinner, more protective corrosion product film, what is lower in overall chlorine, as well as the similar concentration gradients of O and Cl.

Thus the presence of ozone, and its easy reduction, readily provides oxygen to react directly with the Cu (and Ni) and the film from a mixed inner film containing Cl^- ion, to a more efficient barrier layer with a higher fraction of Cu_2O .

The slight decrease in corrosion potentials as ozone concentration are increased to levels greater than -0.2 mg/liter can be explained by the

more rapid production of the barrier layer film, thus inhibiting the cathodic reduction of the ozone.

Stainless Steel

The reaction of ozone with stainless steel in chloride solution appears to be somewhat more complex than that of ozone with actively corroding alloys such as CuNi. As is the case for the copper alloy, the corrosion potential of the stainless steel is shifted in the noble direction by -300 mv. Additionally, even small amounts of ozone (0.016 mg/l) cause the steady state corrosion potential of the stainless steel to reach a steady state value virtually immediately. Increasing the ozone concentration to greater than 0.15 mg/l has no appreciable further effect on the corrosion potential. These results suggest that cathodic reduction of the ozone, as is the case for Cu alloys controls the mixed potential, and that the concentration of ozone is not rate limiting. Rather, only small amounts of ozone are required to react with the stainless steel surface to shift the corrosion potential.

The shift in the breakdown potential, which parallels the shift in the corrosion potential is also interesting in that it appears that the incorporation of oxygen, from the reduction of ozone, stabilizes the film against the initiation of localized corrosion. This apparent improvement in pitting resistance may be related to the rapidity with which passivity is initiated on the alloy surface with dissolved ozone. This is suggested by the lack of correlation of the repassivation potential with ozone concentration, and by the AES results, both of which suggest that the

characteristics of the passive films are not appreciably affected by the presence of ozone in the solution.

However, the marked shift in the corrosion potential in the noble direction with ozonated solutions suggests that crevice corrosion or occluded cell corrosion may be a potential problem for the use of ozone as a biocide in saline solutions. In the ozone concentration range of -0.2 to -0.4 mg/l the measured corrosion potential is equal, to a slightly noble to the repassivation potential, suggesting that while the initiation of localized corrosion may be inhibited, the propagation will be accelerated.

There is an interesting minimum in the measured E_{corr} , E_b , and E_p data a function of O_3 concentration which occurs in the vicinity of 0.3 mg/l dissolved O_3 . Since the E_{corr} and polarization experiments were independently conducted, it is believed that this minimum is a valid observation. However, its origin is, at this time unknown, although it may be related to larger potential differences between the passive surface and actively growing pits because of the higher oxidation state of the surface. Larger concentrations of ozone may mask this minimum because of a stronger ability to repassivate small initiated pits.

Conclusions

1. The addition of ozone to chloride solutions results in a noble shift in the corrosion potential of both Cu-30Ni and 304L stainless steel. This shift in corrosion potential is virtually instantaneous in contrast to a significant transient period to achieve a steady state potential in solutions which do not contain ozone. The corrosion potential of both alloys in ozonated solutions is almost independent of ozone concentrations for concentrations greater than ~ 0.2 mg/liter.

2. For Cu-30 Ni the presence of dissolved ozone results in a thinner film containing a higher fraction of oxygen to chloride than for unozonated solutions. This corrosion product film results in a decrease in corrosion susceptibility as measured by current density at fixed potentials.

3. For 304L stainless steel, a shift in the breakdown potential in the noble direction occurs, suggesting that ozone inhibits the initiation of localized corrosion. On the other hand, the repassivation potential is virtually unchanged by dissolved ozone, and the noble shift in the corrosion potential which is a result of the ozone renders the alloy more susceptible to the possibility of crevice corrosion if appropriate geometries are present. Ozone concentrations on the order of $0.2 - 0.3$ mg/l appear to present the most dangerous conditions for the propagation of crevice corrosion. The chemistry of the passive film, as determined by Auger electron spectroscopy, is apparently not affected by the presence of dissolved ozone in chloride solutions.

Acknowledgments

The support of the Office of Naval Research and particularly of Dr. A.J. Sedriks under contract N00014-86-K-0194 is gratefully acknowledged.

References

1. R. Francis, in Stainless Steels '87, p. 192, 1988, The Institute of Metals, London.
2. R.E. Malpas, P. Gallagher and E.B. Shone, in Stainless Steels '87, p. 253, 1988, The Institute of Metals, London.
3. J.A. Manning and S.V. Carleton, Materials Performance, 14(8), p. 1975.
4. J. Valkering, Corrosion, 6, 123 (1950).
5. W.C. Steward and F.L. LeQue, Corrosion, 8, 269 (1952).
6. R.J. Furara, L.E. Tauschenberg and P.J. Moran, Paper #211, Corrosion '85, NACE, Houston, Texas, 1985.
7. M. Matsudaira, M. Suzuki and Y. Sato, Materials Performance, 21(11), p. 55, 1981.
8. Standard Methods for the Examination of Water and Wastewater, 15th ed., M.A.H. Franson, Ed. Am. Public Health Assoc.
9. K. Efird, Corrosion, 31, 77, 1975.

Table 1. Chemical Composition of the Alloys Used in This Study

70Cu-30Ni

Cu	Pb	Fe	S	P	Ni	Zn	C
68.55	0.008	0.548	0.007	0.006	30.0	0.109	0.035

304L Stainless Steel

C	Mn	P	S	Cr	Ni	Cu	N	Co	Si	Mo
0.016	1.55	0.009	0.016	18.82	9.72	0.10	0.04	0.10	0.70	0.05

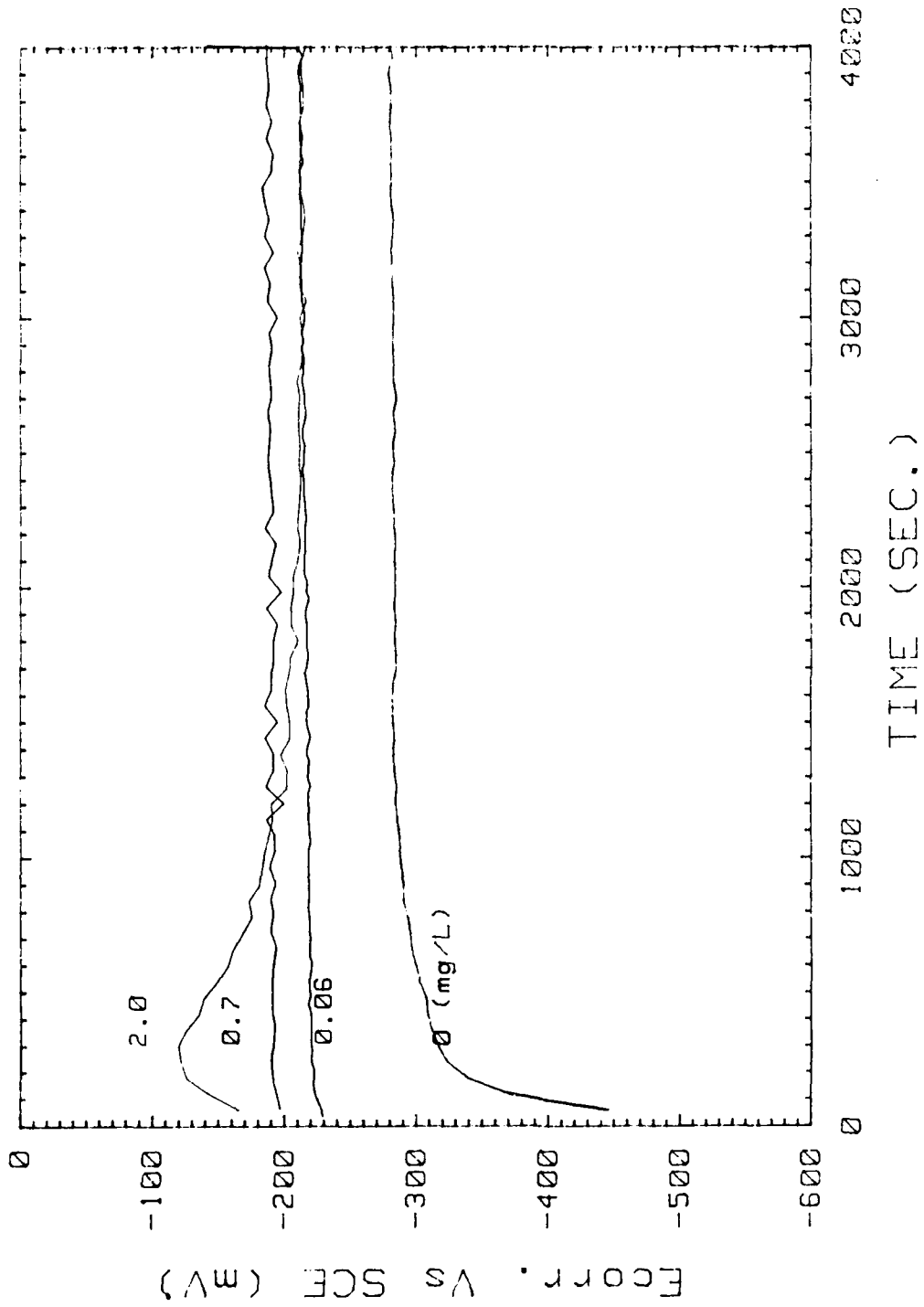


Fig.1 Corrosion potential (E_{corr.}) versus time for 70Cu-30Ni alloy in 0.5N NaCl solution (PH=5) as a function of ozone concentration.

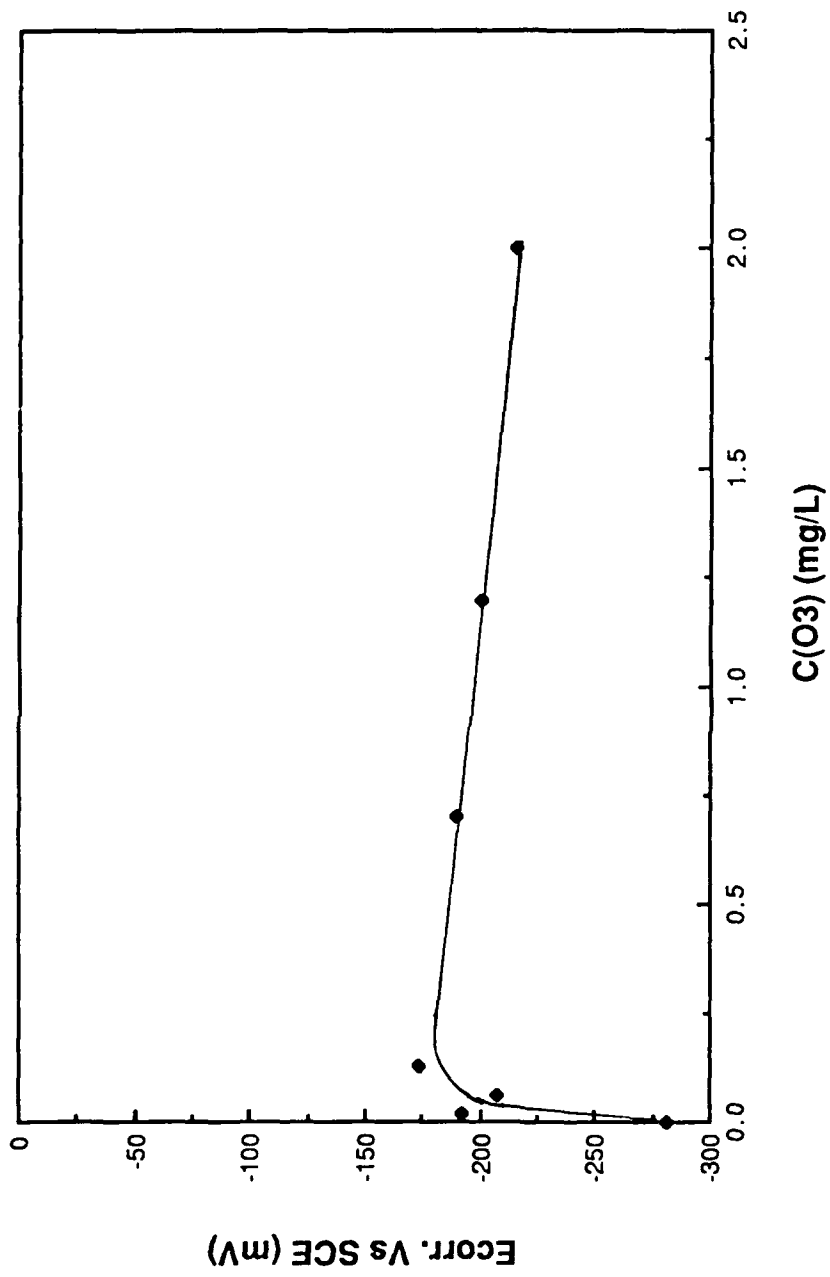


Fig. 2 The corrosion potential as a function of ozone concentration for a 70Cu-30Ni alloy in 0.5N NaCl solution.

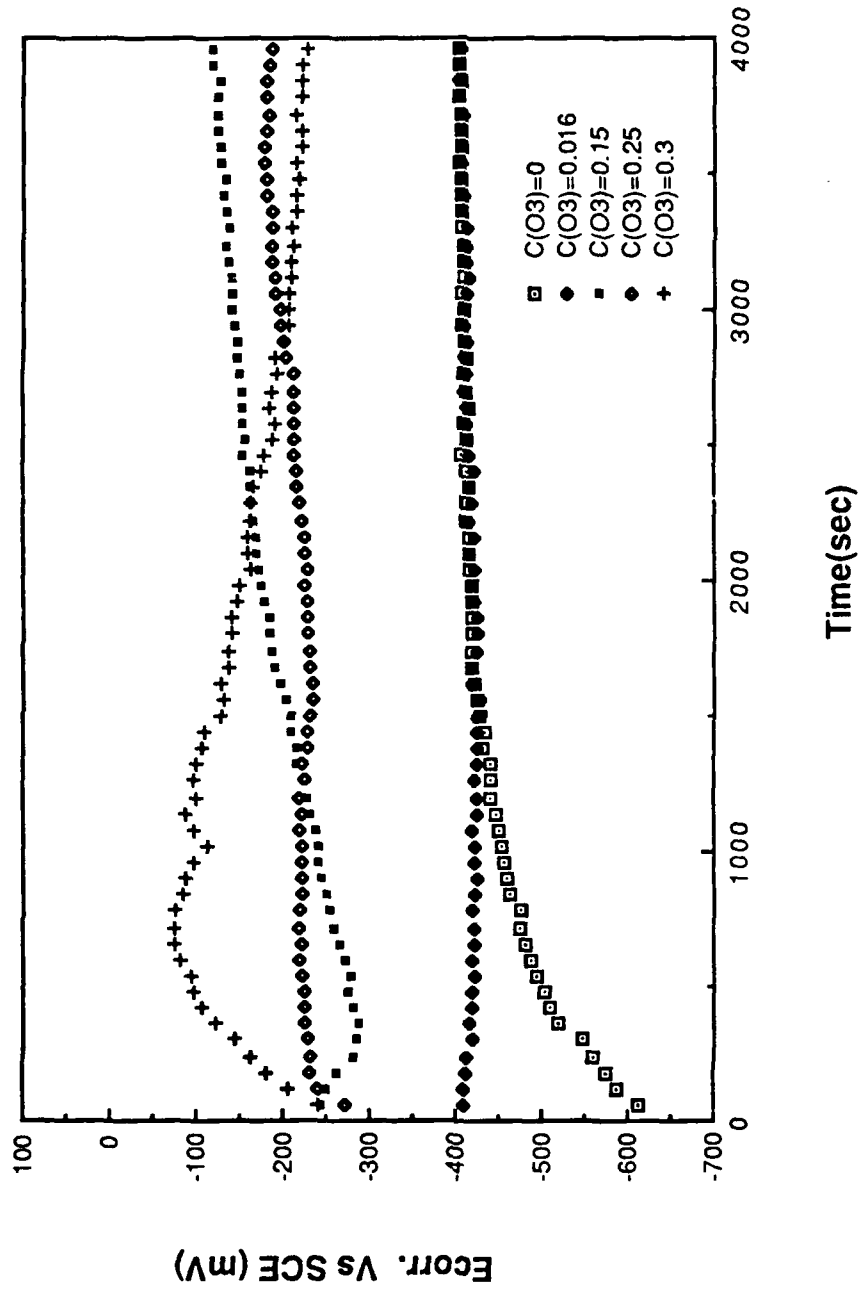


Fig.3a Corrosion potential (E_{corr.}) versus time for 304L stainless steel in 0.5N NaCl solution (PH=5) as a function of ozone concentration (0-0.3 mg/L).

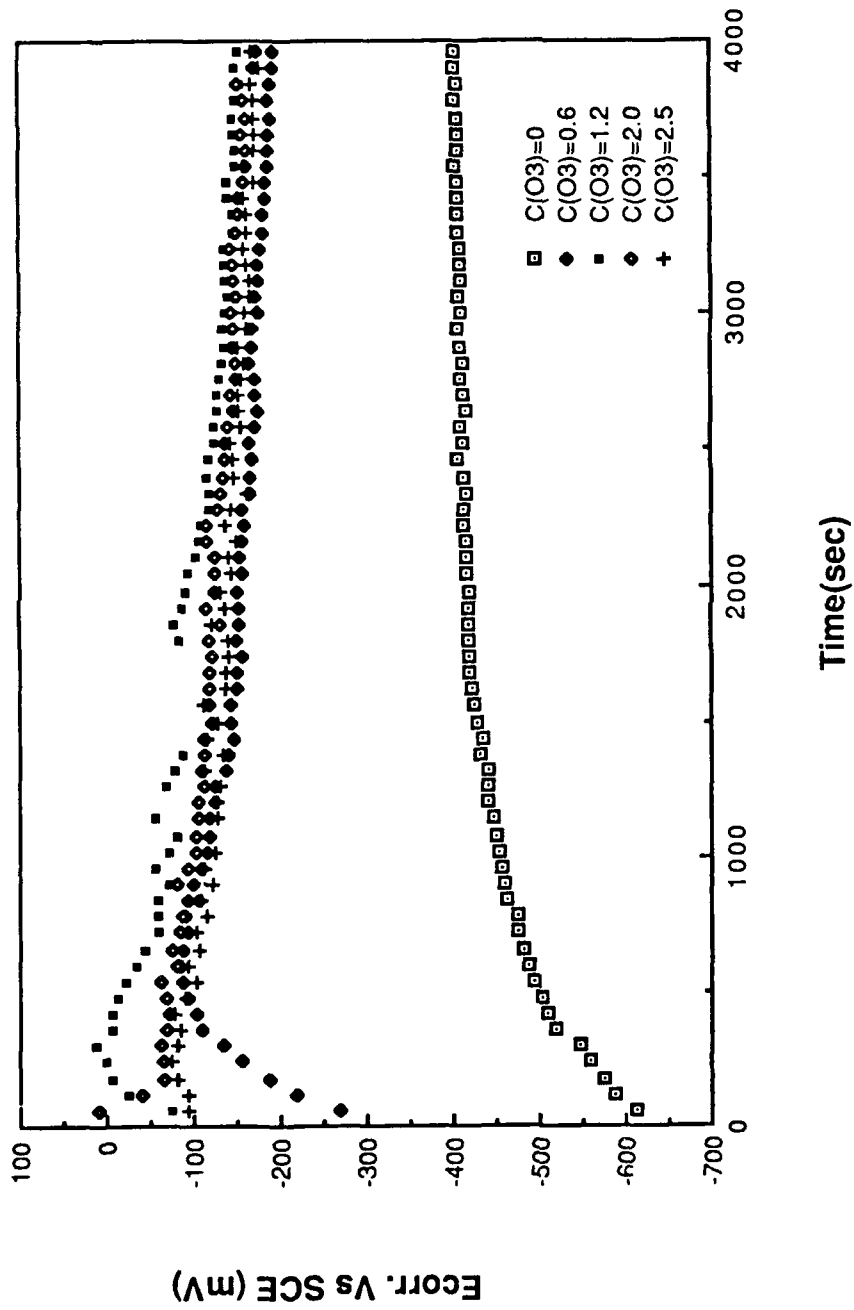


Fig.3b Corrosion potential (E_{corr.}) versus time for 304L stainless steel in 0.5N NaCl solution (PH =5) as a function of ozone concentration (0.6-2.5 mg/L).

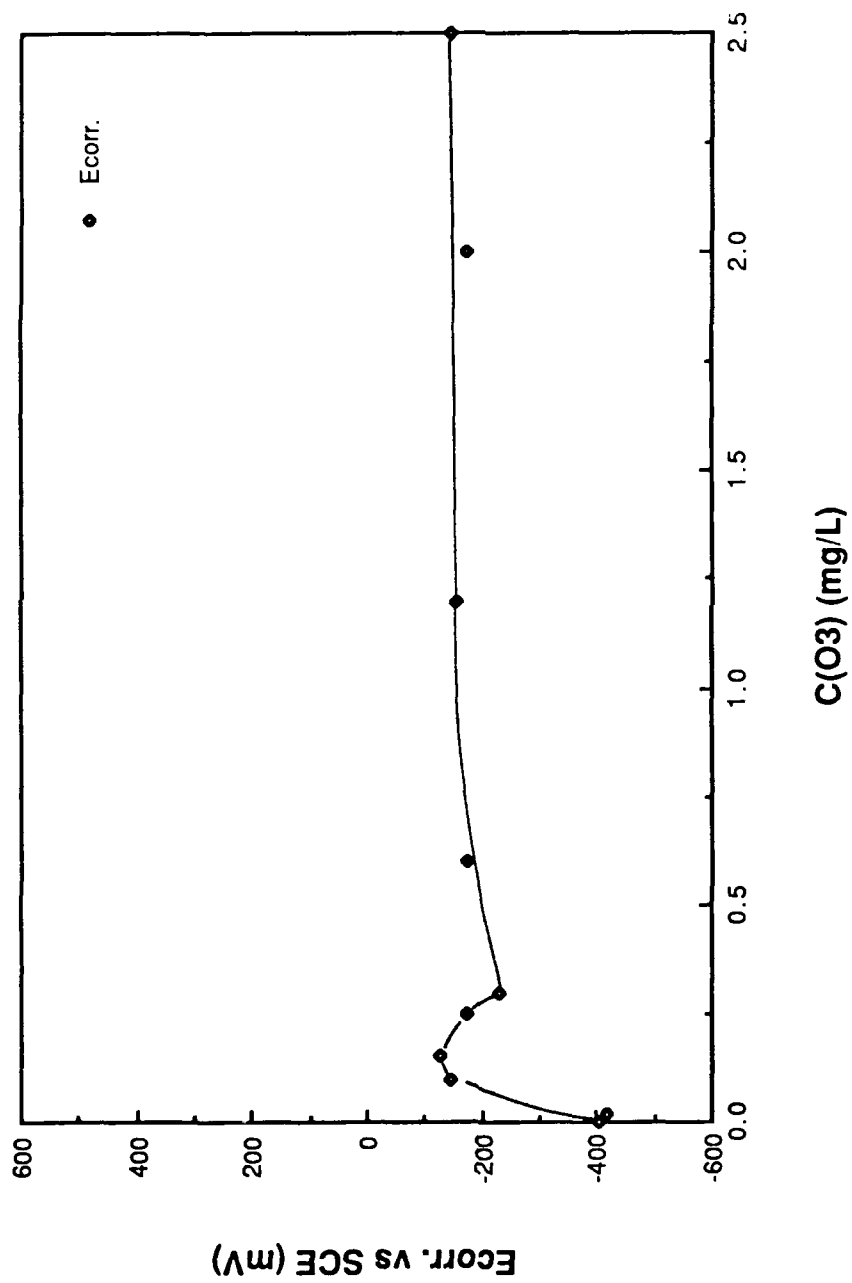


Fig. 4 The effect of ozone concentration on $E_{corr.}$ in 0.5N NaCl solution for 304L stainless steel.

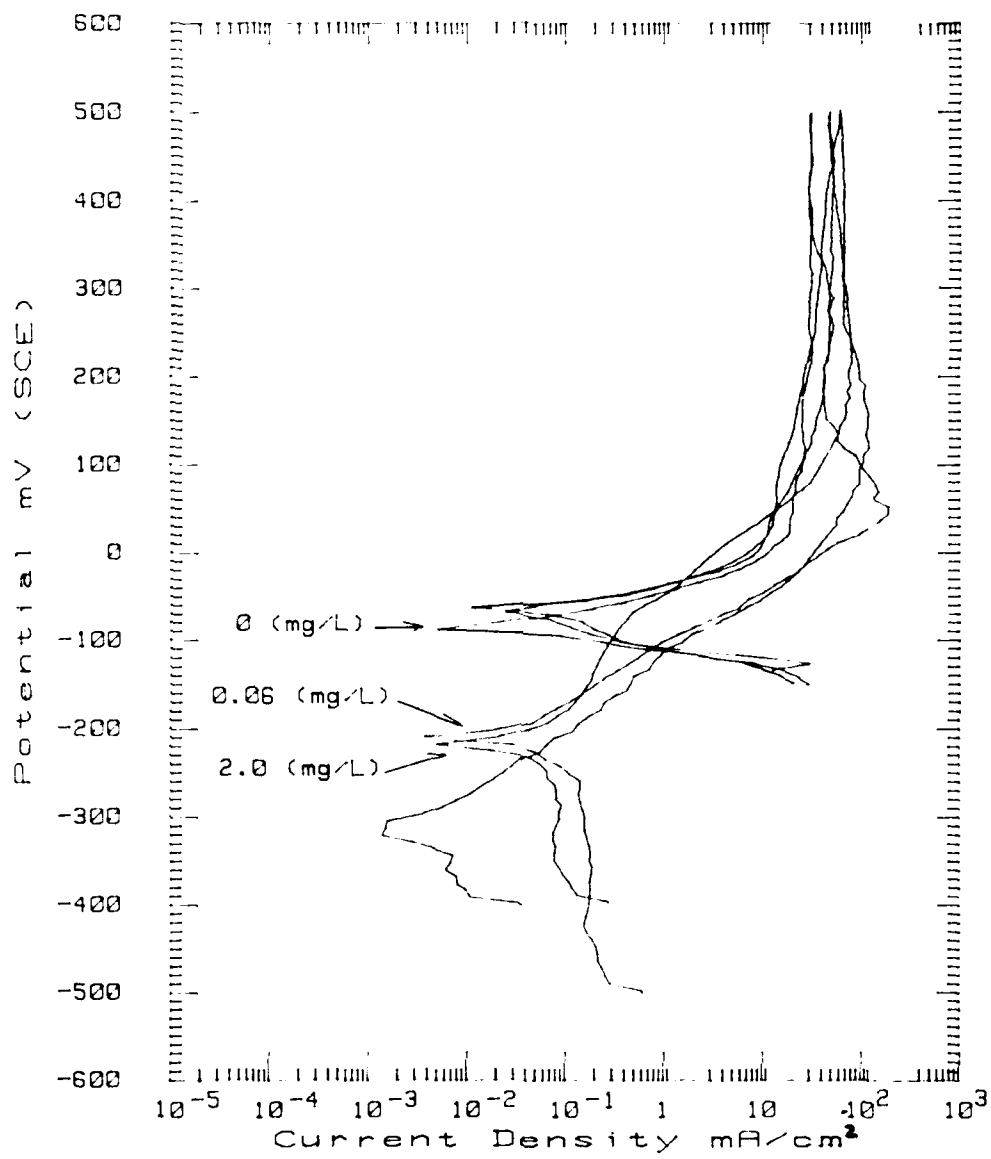


Fig.5 Cyclic polarization curves for 70Cu-30Ni alloy in 0.5N NaCl solution as a function of ozone concentration.

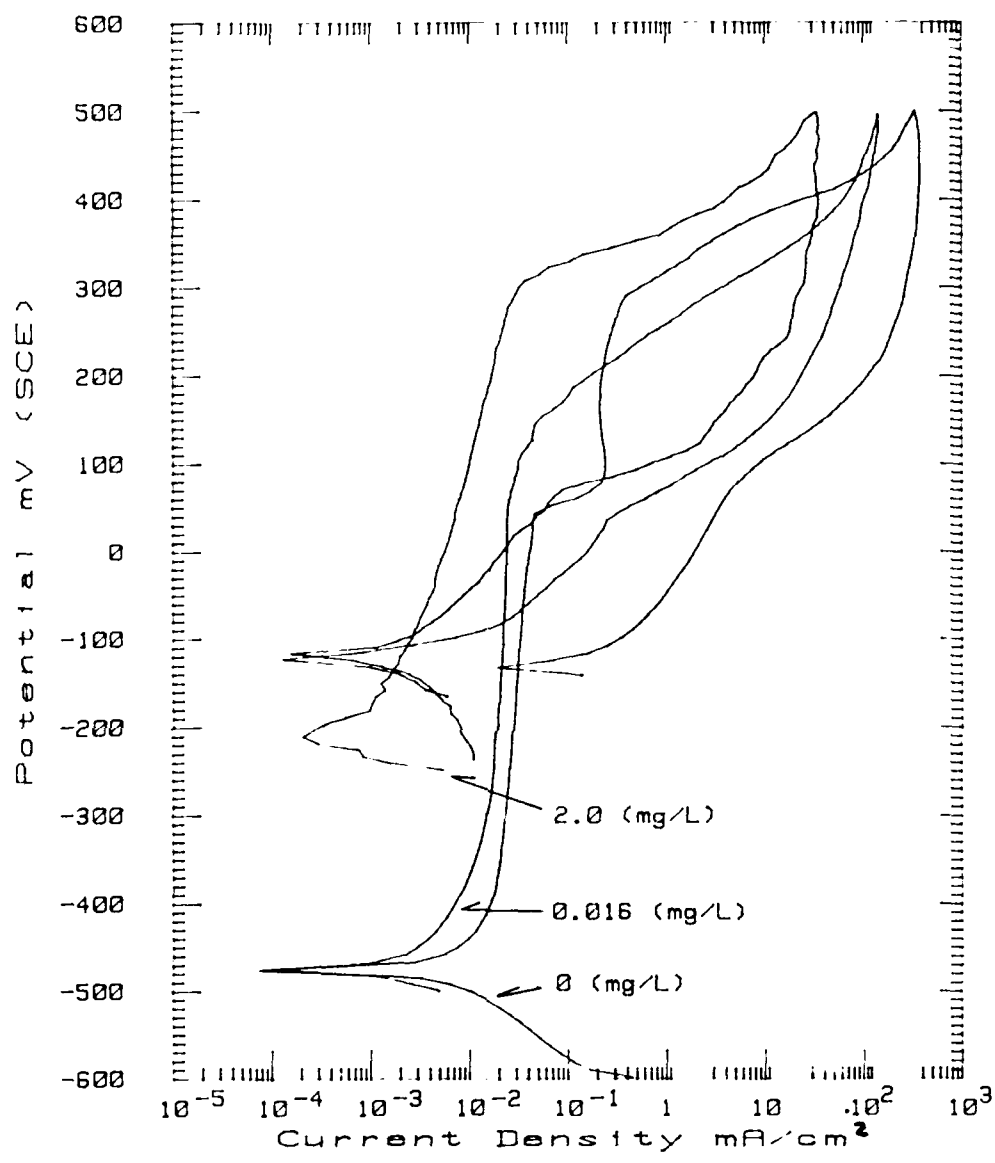


Fig.6 Cyclic polarization curves for 304L stainless steel in 0.5N NaCl solution as a function of ozone concentration.

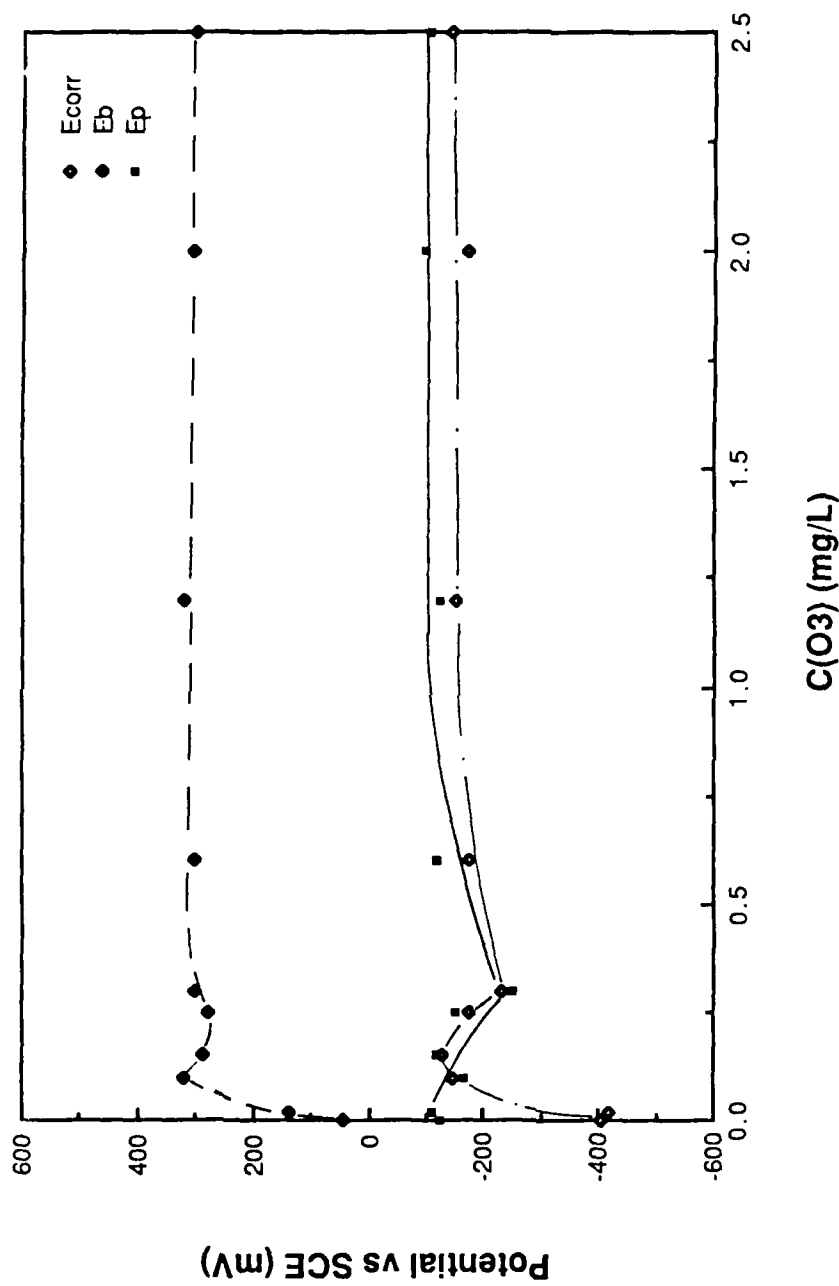


Fig. 7 The effect of ozone concentration on the breakdown potential (Eb) and repassivation potential (Ep) in 0.5N NaCl solution for 304L stainless steel.

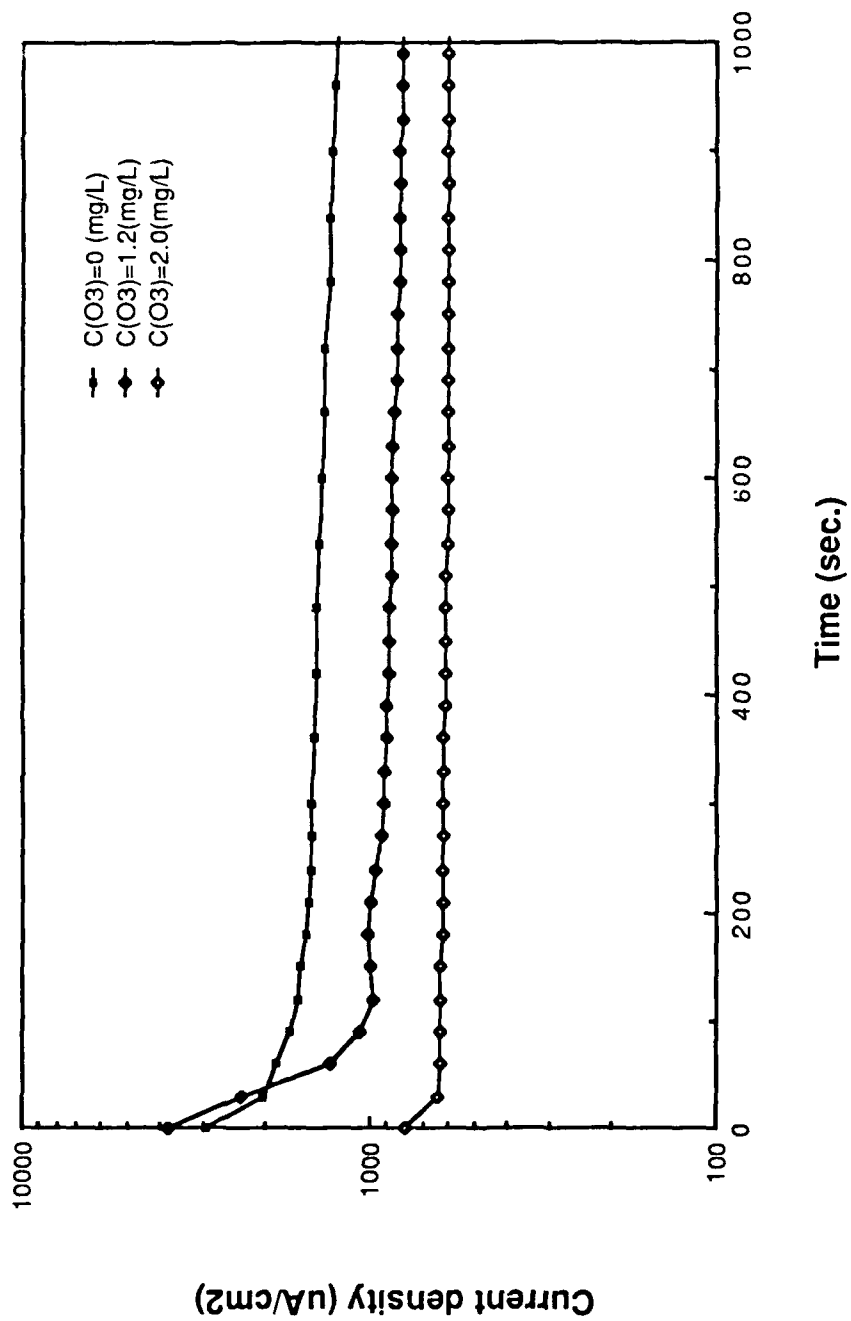


Fig. 8 Current density vs time as a function of ozone concentration for 70Cu-30Ni in 0.5N NaCl solution, $E_{app} = 100$ mV vs SCE.

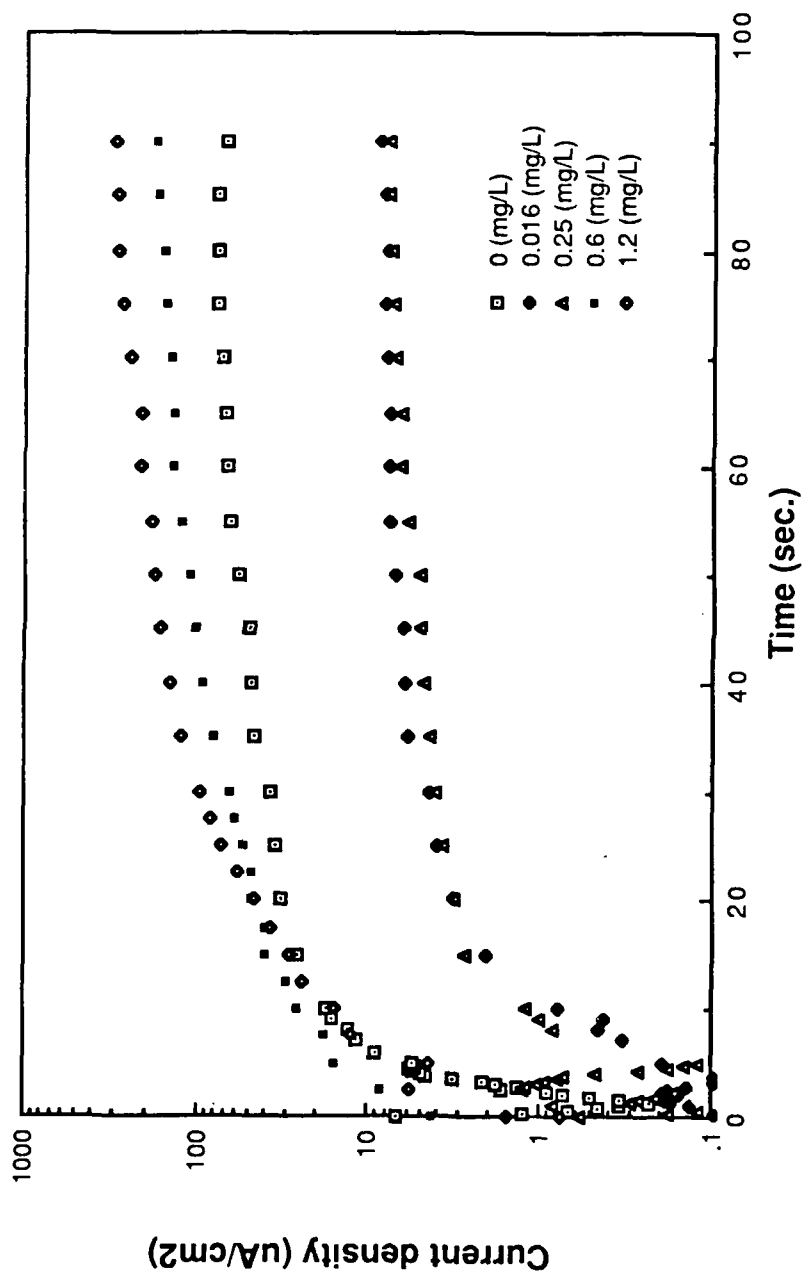


Fig. 9 Current density vs time as a function of ozone concentration for 304L stainless steel in 0.5N NaCl solution, $E_{app} = 100$ mV vs SCE.

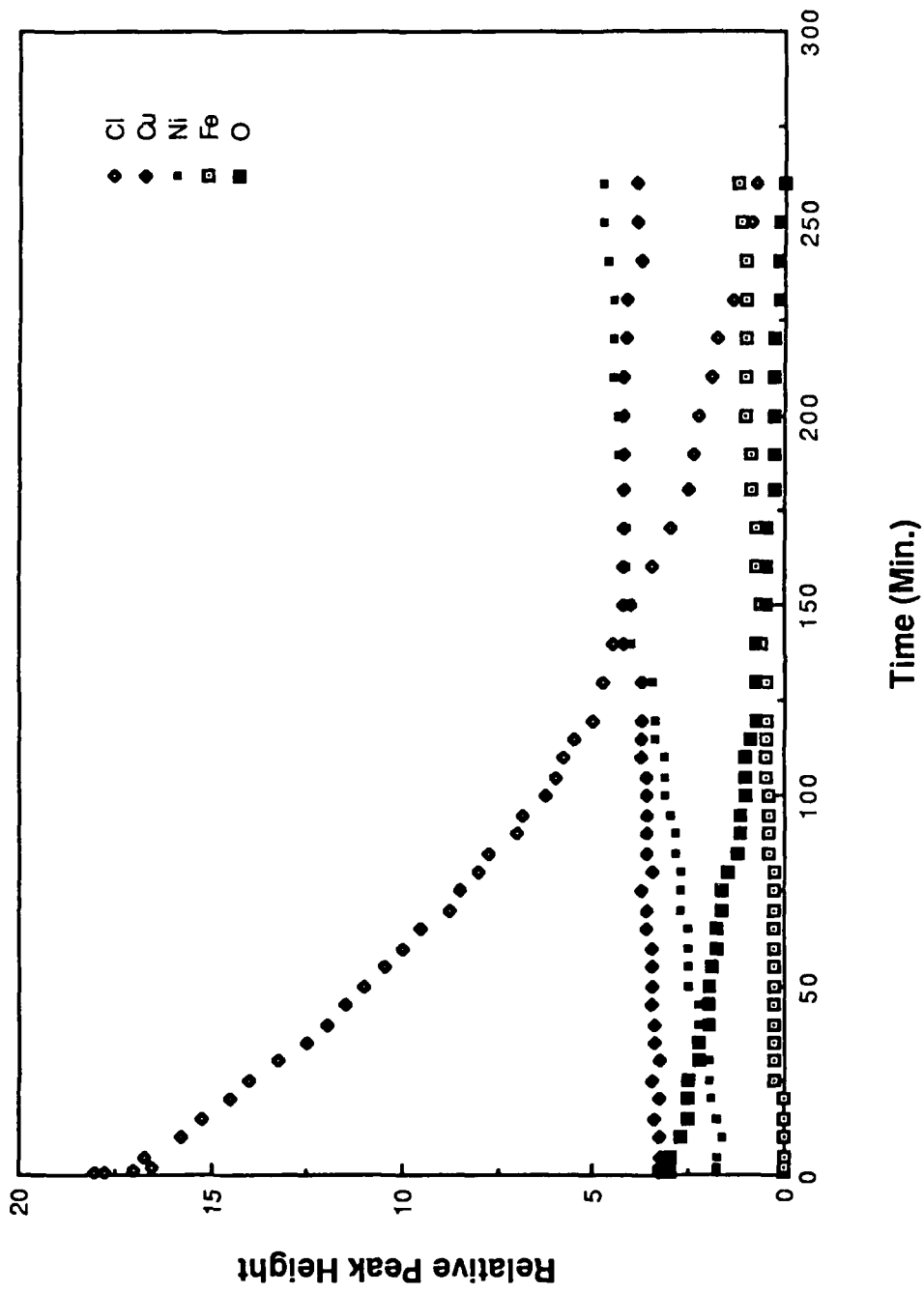


Fig. 10a Depth profiling by AES on a 70Cu-30Ni alloy in 0.5N NaCl solution (0 mg/L ozone), sputtering rate = 10 A/Min..

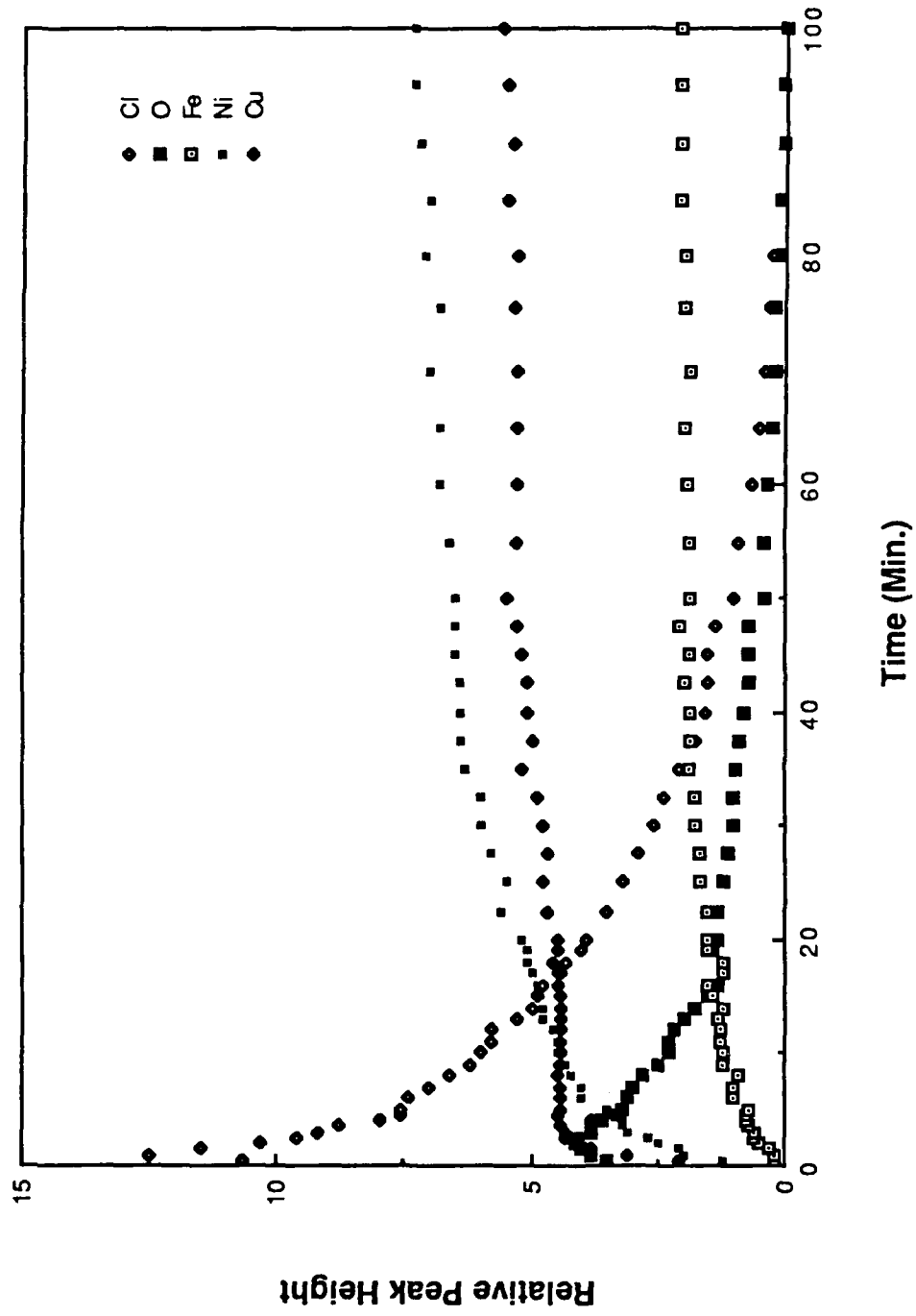


Fig. 10b Depth profiling by AES on a 70Cu-30Ni alloy in 0.5N NaCl solution (0.6 mg/L ozone), sputtering rate = 10 A/Min..

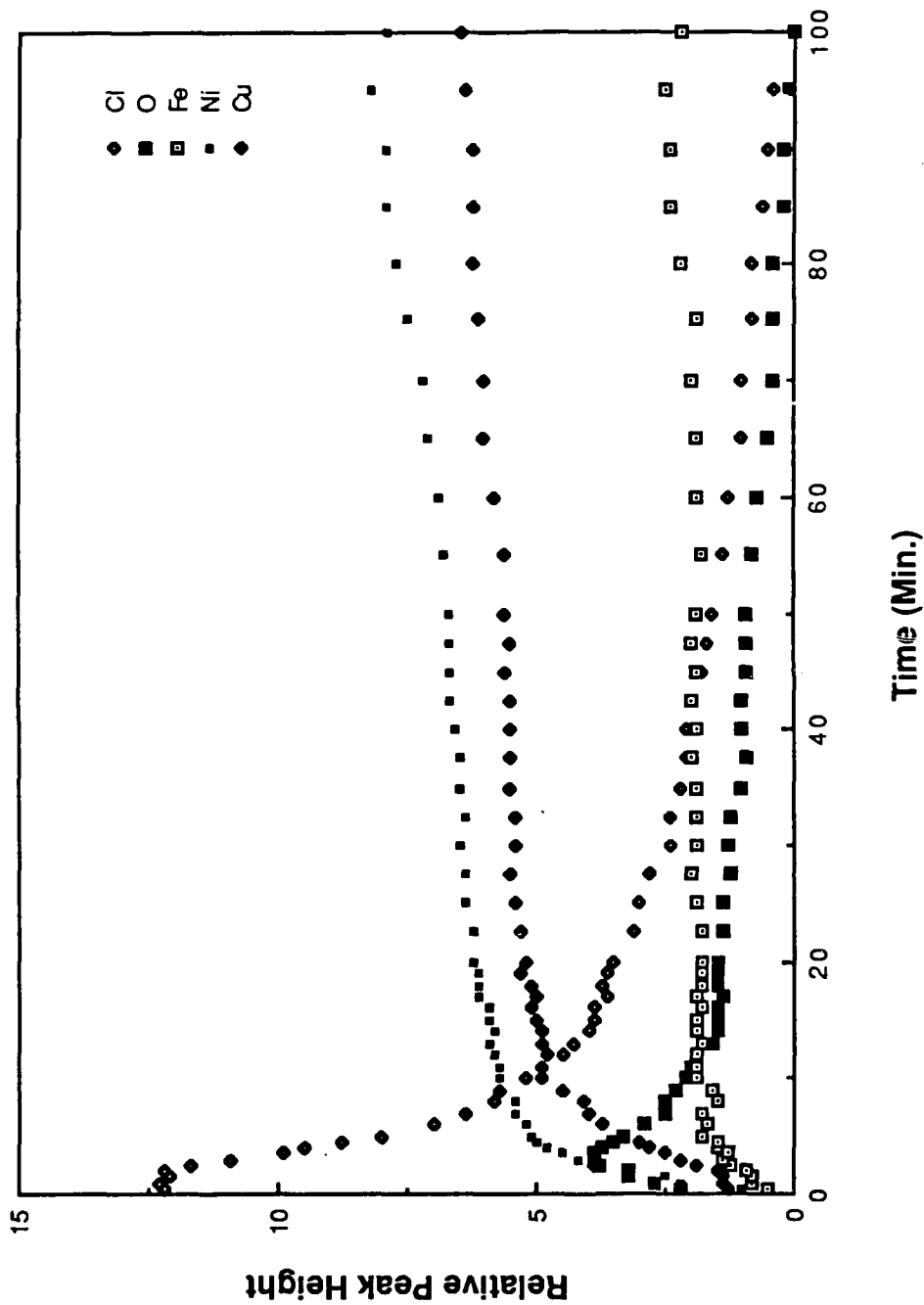


Fig. 10c Depth profiling by AES on a 70Cu-30Ni alloy in 0.5N NaCl solution (2.0 mg/L ozone), sputtering rate = 10 A/Min..

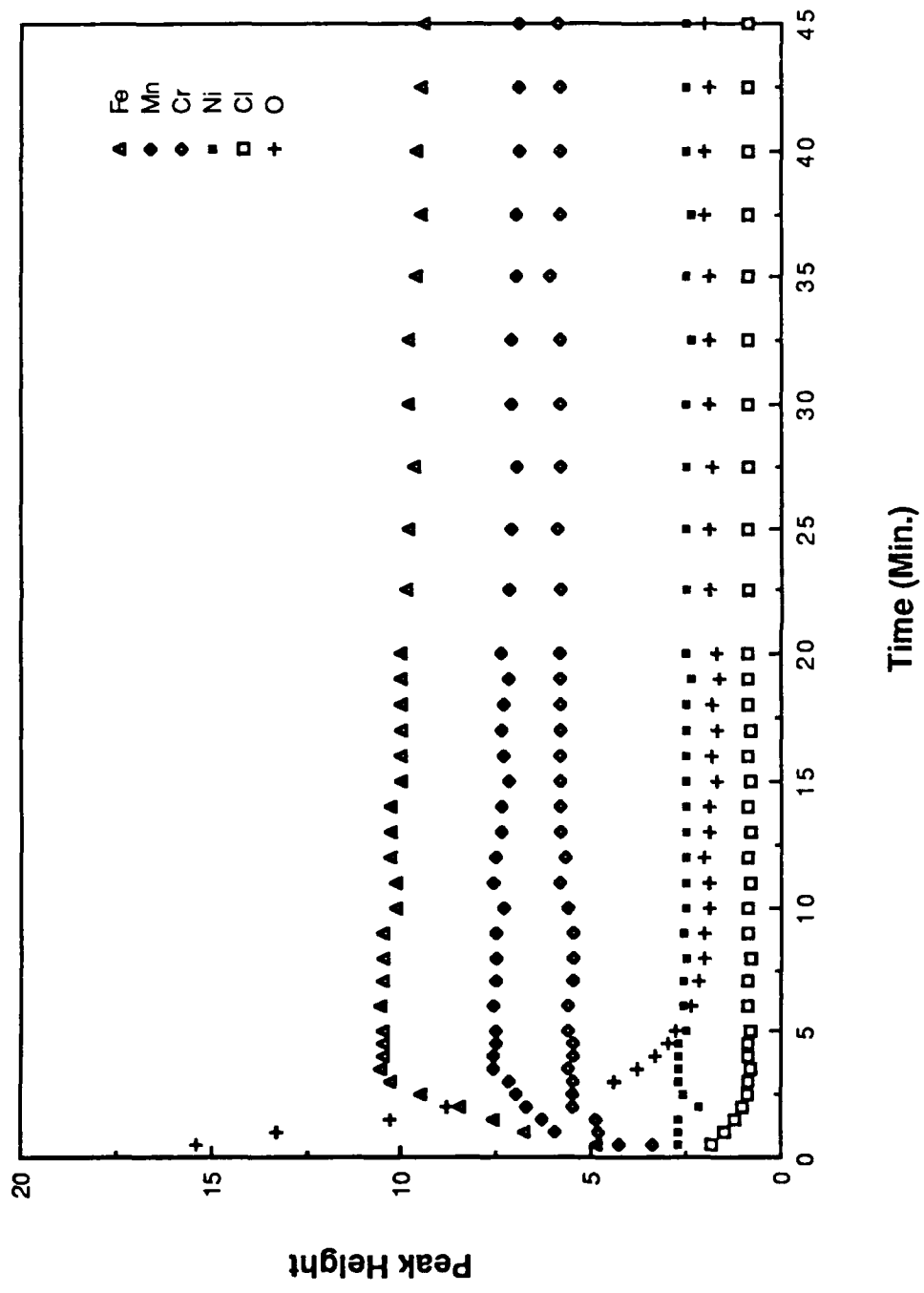


Fig. 11a Depth profiling by AES on 304L S S alloy exposed in 0.5N NaCl solution (0 mg/L ozone), sputtering rate = 10 A/Min..

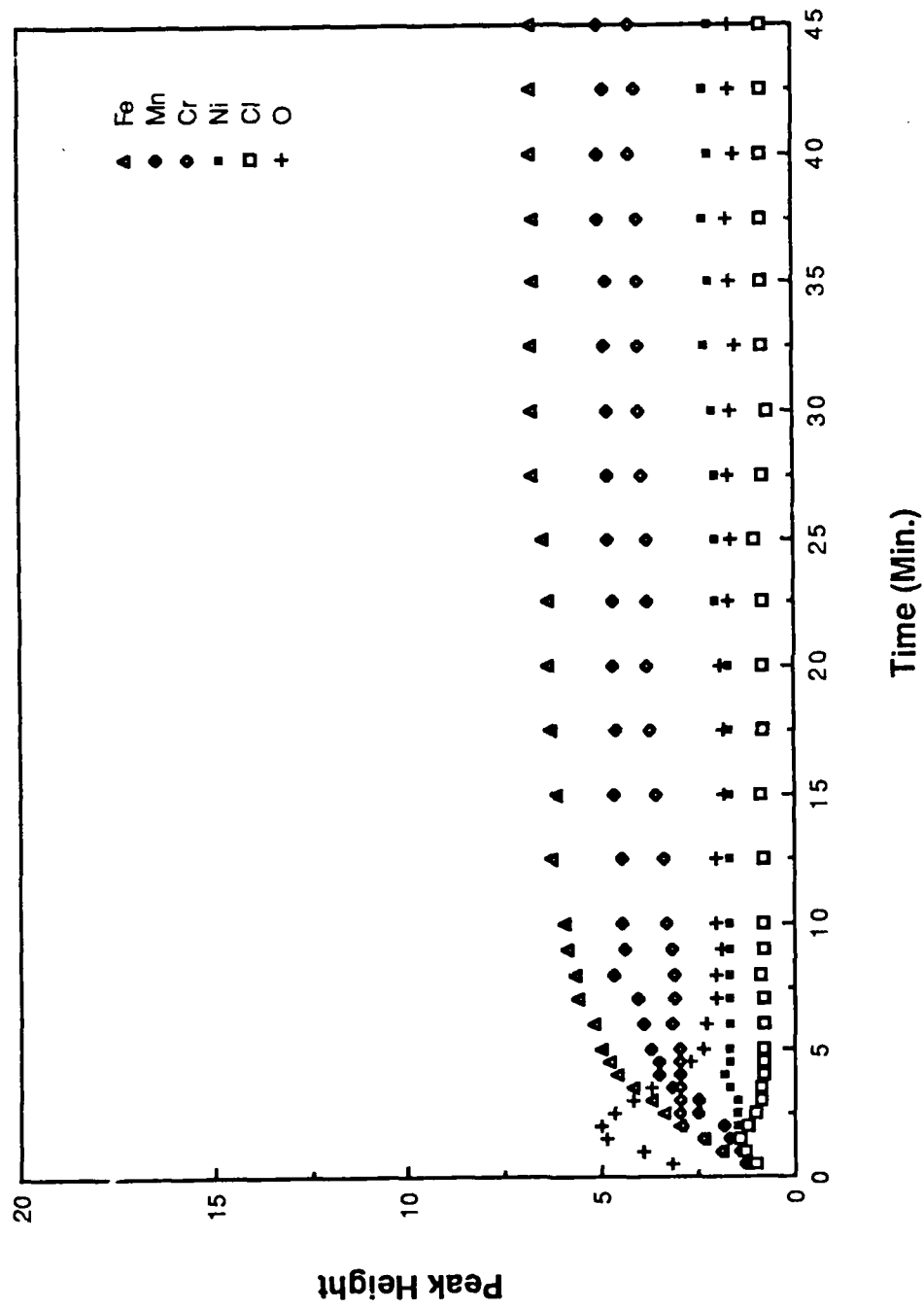


Fig. 11b Depth profiling by AES on 304L S S alloy exposed in 0.5N NaCl solution (0.1 mg/L ozone), sputtering rate = 10 A/Min..

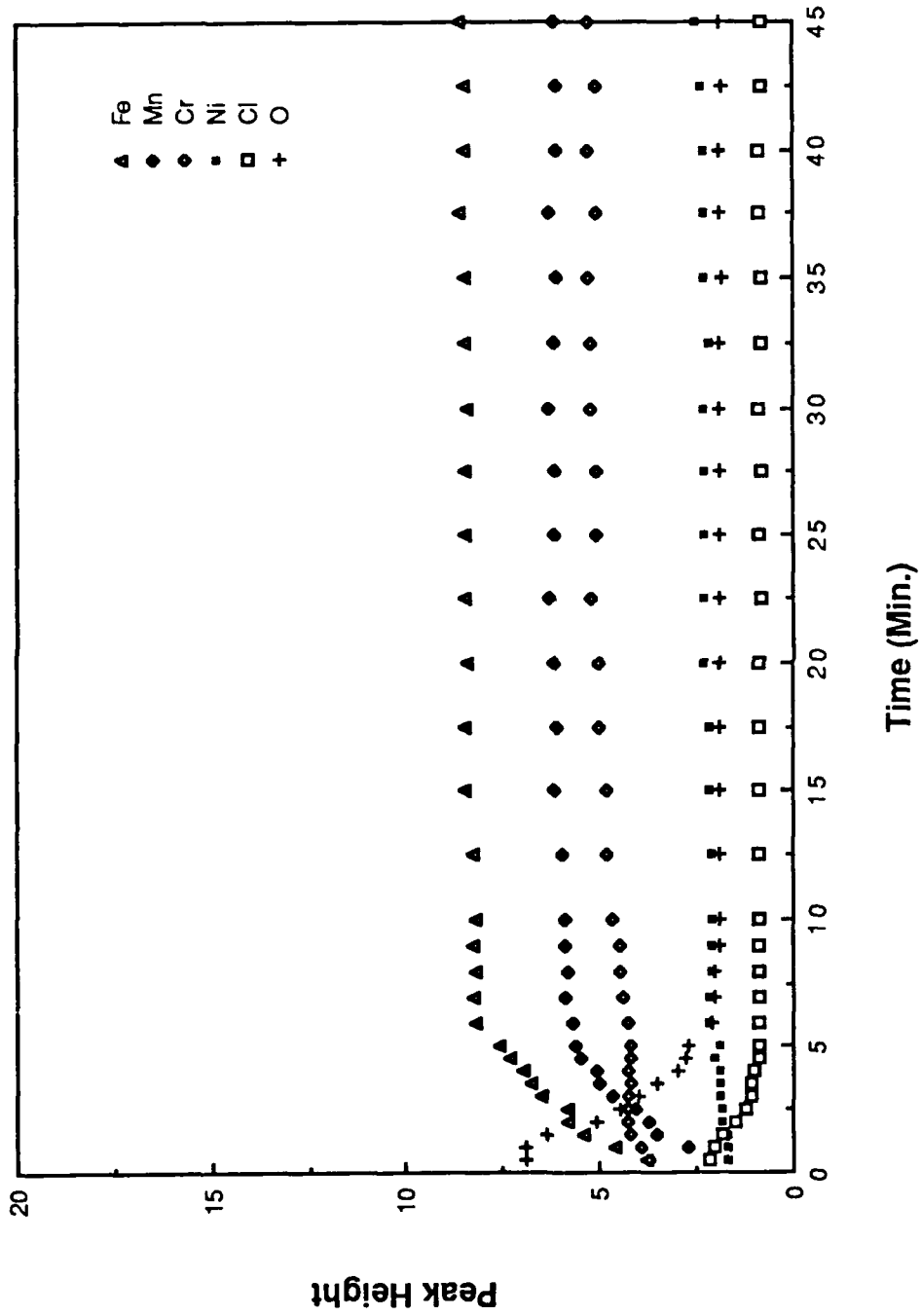


Fig. 11c Depth profiling by AES on 304L S S alloy exposed in 0.5N NaCl solution (2.5 mg/L ozone), sputtering rate = 10 A/Min..

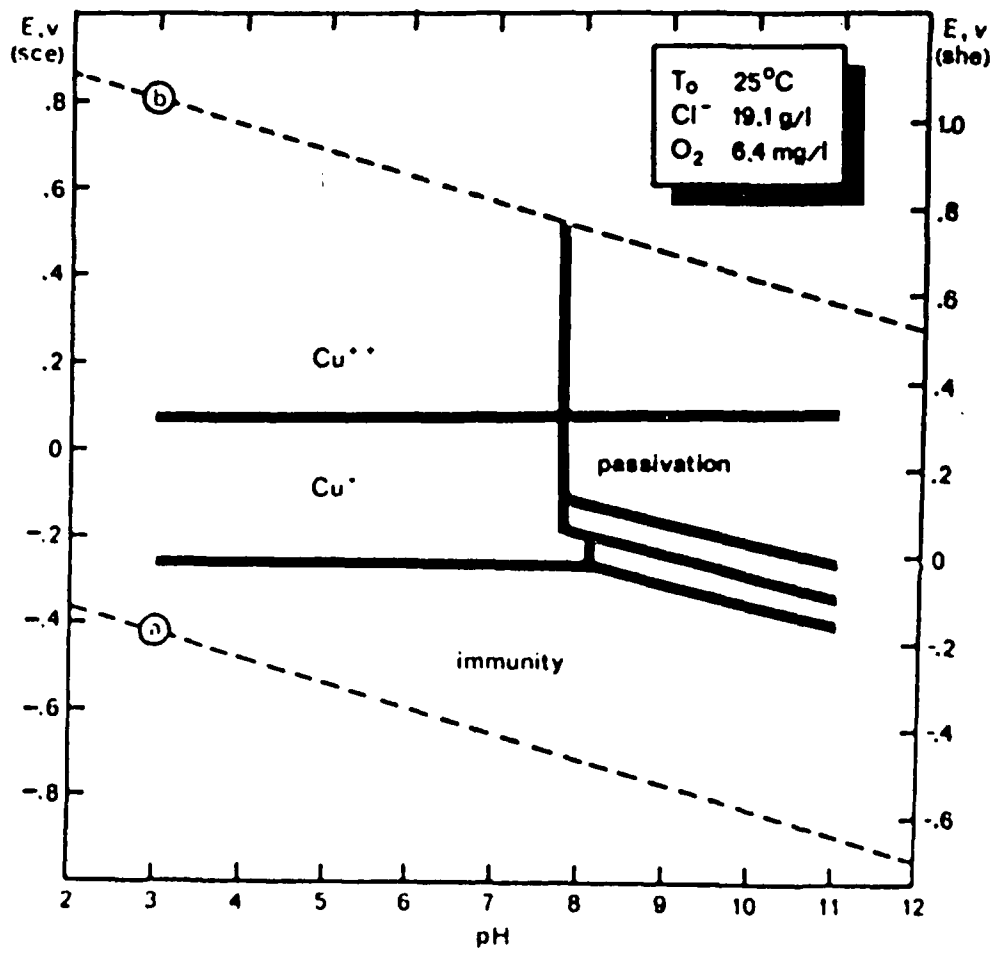


Fig.12 A simplified potential-pH diagram for
 70Cu-30Ni in seawater ⁽⁹⁾ .

REPORT DOCUMENTATION PAGE

1a. REPORT SECURITY CLASSIFICATION Unrestricted			1b. RESTRICTIVE MARKINGS None		
2a. SECURITY CLASSIFICATION AUTHORITY			3. DISTRIBUTION/AVAILABILITY OF REPORT Unrestricted		
2b. DECLASSIFICATION/DOWNGRADING SCHEDULE					
4. PERFORMING ORGANIZATION REPORT NUMBER(S) 2			5. MONITORING ORGANIZATION REPORT NUMBER(S)		
6a. NAME OF PERFORMING ORGANIZATION Rensselaer Polytechnic Institute		6b. OFFICE SYMBOL (If applicable)	7a. NAME OF MONITORING ORGANIZATION		
6c. ADDRESS (City, State and ZIP Code) Try, NY 12180-3590			7b. ADDRESS (City, State and ZIP Code)		
8a. NAME OF FUNDING/SPONSORING ORGANIZATION Office of Naval Research		8b. OFFICE SYMBOL (If applicable)	9. PROCUREMENT INSTRUMENT IDENTIFICATION NUMBER		
8c. ADDRESS (City, State and ZIP Code) 800 N. Quincy Street Arlington, VA 22217-5000			10. SOURCE OF FUNDING NOS.		
			PROGRAM ELEMENT NO.	PROJECT NO.	TASK NO.
					WORK UNIT NO.
11. TITLE (Include Security Classification) The Effect of Dissolved Ozone on the Corrosion Behavior of Cu-30 Ni and 304L Stainless Steel in 0.5 N NaCl Solutions					
12. PERSONAL AUTHOR(S) H.H. Lu and D.J. Duquette					
13a. TYPE OF REPORT Technical		13b. TIME COVERED FROM 10/86 TO 10/89		14. DATE OF REPORT (Yr., Mo., Day) 89 10 15	15. PAGE COUNT 37
16. SUPPLEMENTARY NOTATION NONE					
17. COSATI CODES			18. SUBJECT TERMS (Continue on reverse if necessary and identify by block number) Corrosion, Stainless Steel, Copper Nickel Alloy, Dissolved Ozone, chloride Solutions		
FIELD	GROUP	SUB. GR.			
19. ABSTRACT (Continue on reverse if necessary and identify by block number) Electrochemical experiments on the effect of dissolved ozone on the corrosion behavior of Cu-30 Ni and 304 L stainless steel have been performed in 0.5 N NaCl solutions at room temperature. The experiments performed included measurements of corrosion potential as a function of time and ozone concentrations, cyclic polarization experiments, iso-potential measurements of current densities and Auger electron spectroscopy studies of the chemical composition of the corrosion product films. The results of these experiments have shown that for both the Cu-based alloy and the stainless steel, the corrosion potential exhibits a marked shift to more noble values (~300 mv) for ozone concentrations less than 0.2 - 0.3 mg/l. At higher ozone concentrations the corrosion potential is virtually independent of the level of ozone dissolved in the solution. In addition to the shift in the corrosion potential, the presence of dissolved ozone resulted in a reduction in the corrosion rate for the Cu-30 Ni alloy, as measured by a significant decrease in the current density at a constant applied (SEE BACK PAGE)					
20. DISTRIBUTION/AVAILABILITY OF ABSTRACT UNCLASSIFIED/UNLIMITED <input checked="" type="checkbox"/> SAME AS RPT. <input type="checkbox"/> DTIC USERS <input type="checkbox"/>			21. ABSTRACT SECURITY CLASSIFICATION Unrestricted		
22a. NAME OF RESPONSIBLE INDIVIDUAL D.J. Duquette			22b. TELEPHONE NUMBER (Include Area Code) 518-276-6459		22c. OFFICE SYMBOL

potential. This improvement in the corrosion resistance appears to be related to a reduction in the corrosion product film thickness and a higher fraction of oxygen to chloride in the corrosion product film.

For the stainless steel, on the other hand, Auger electron spectroscopy indicated no appreciable differences between the passive film produced in oxonated solutions versus those in unozonated solutions. However, the noble shift in the corrosion potential was accompanied by a parallel shift in the breakdown potential, suggesting that films produced in ozonated solutions are more resistant to the initiation of localized corrosion. However, the repassivation potential of the stainless steel is not perceptibly changed by dissolved ozone and the corrosion potential approached the repassivation potential. This results in the rapid propagation of pits once they have initiated.